Relativistic Brueckner-Hartree-Fock Theory: an ab initio Approach for Nuclear Matter and for Finite Nuclei

Peter Ring
Department of Physics, Technische Universität München, D-85747 Garching, Germany
Exzellenzcluster ORIGINS, Boltzmannstr. 2, D-85748 Garching, Germany

Sibo Wang
Department of Physics, Chongqing University, Chongqing 401331, China

Hui Tong
College of Physics and Materials Science, Tianjin Normal University, Tianjin 300387, China
Strangeness Nuclear Physics Laboratory, RIKEN Nishina Center, Wako, 351-0198, Japan

Qiang Zhao
Center for Exotic Nuclear Studies, Institute for Basic Science, Daejeon 34126, Korea

Chencan Wang
School of Physics, Nankai University, Tianjin 300071, China

Jie Meng
State Key Laboratory of Nuclear Physics and Technology, School of Physics,
Peking University, Beijing 100871, China
Yukawa Institute for Theoretical Physics, Kyoto University, Kyoto 606-8502, Japan

E-mail: peter.ring@tum.de

Abstract. Recent years have seen considerable progress with ab-initio calculations of the nuclear structure by non-relativistic many-body methods. Dirac-Brueckner-Hartree-Fock Theory provides a relativistic ab-intio approach, which is able to reproduce saturation properties of symmetric nuclear matter without three-body forces. However, so far, the corresponding equations have been solved only for positive energy states. Negative energy states have been included for forty years in various approximations, leading to differences in the isospin dependence. This problem has been solved only recently by a complete solution of the self-consistent relativistic Brueckner-Hartree-Fock equations in asymmetric nuclear matter. Due to its numerical complexity, however, it is very difficult to extend the Relativistic Brueckner-Hartree-Fock theory to the study of finite nuclear systems. Recent efforts will be discussed to overcome this problem.

1. Introduction

In the last thirty years ab-initio derivations of nuclear structure properties are at the forefront of nuclear studies. Here the starting point are bare nucleon-nucleon forces. They are used to calculate binding energies, radii, and spectroscopic data. Nowadays it is possible to solve the exact nuclear many-body problem for light nuclei on the computer. Investigations of properties for the majority of nuclear systems, however, are carried out in the framework of density functional theory. Non-relativistic [1, 2] and relativistic [3, 4, 5, 6, 7, 8] versions allow a successful description of the nuclear many-body problem not only for ground state properties, but also for excitations such as collective rotations and giant resonances and, by going beyond mean field, for sophisticated low-lying spectra in transitional nuclei [9, 10] and the coupling to complex configurations [11]. At present most of these functionals contain phenomenological parts. Therefore, one of the main goals in nuclear structure physics is to derive a universal density functional based on microscopic calculations [12, 13], a goal which has been reached since many years in Coulombic systems [14]. This functional should allow to explain as many data as possible within a universally valid parameter set and to provide reliable predictions for nuclei far from stability, which are at present not accessible to experiments in the laboratory. It should be derived in a completely microscopic way from the bare interactions. At present, however, such attempts provide only qualitative results for two reasons: first, the three-body term of the bare interaction is not known well enough and, second, the methods to derive such a functional are not precise enough to achieve the required accuracy.

In deriving such energy density functionals, symmetries play an essential role. One of the underlying symmetries of QCD is Lorentz invariance. Therefore, in nuclear physics, relativistic density functionals are of particular interest. This symmetry allows consistently describing the spin-orbit coupling. It has an important influence on the underlying shell structure. In addition, it puts many restrictions on the number of parameters in the corresponding functionals but keeps the quality of the agreement with experimental data [8]. The velocities of nucleons in the Fermi sea are relatively small. However, as sumrule approaches to QCD predict [15], there are large scalar and vector fields of opposite sign in the nuclear medium. Since the fifties, one knows [16] that they cancel in the average field, but they add up in the velocity-dependent spin-orbit term, such that even small velocities lead to significant effects. They are difficult to handle in perturbation theory. A non-relativistic expansion is possible, but it leads to various large correction terms at the cost of additional phenomenological parameters in non-relativistic density functionals. Therefore we restrict ourselves, in the following, to Covariant Density Functionals Theory (CDFT).

2. Semi-microscopic density functionals

In Coulombic systems an essential input for the derivation of microscopic functionals [14] is the numerical calculation of the energy of an homogeneous electron gas as a function of the density. Starting from this energy functional $E_\infty[\rho]$ additional corrections are added with great success. It seems to be reasonable to apply a similar concept in nuclear physics [22]. Of course, at present, there are no exact solutions for homogeneous nuclear matter available. One has to rely on approximate solutions, such as sophisticated variational calculations [23] or modern Brueckner-Hartree-Fock methods [17, 18]. The point coupling functional DD-PC1 of the Munich-Zagreb group [21] used this microscopic input together with experimental masses of 64 heavy deformed nuclei. Ten phenomenological parameters have been adjusted, four coupling constants at saturation densities: α_S, α_V, α_{ST}, δ_S and six additional parameters to describe the density dependence. The result is a semi-microscopic functional with an equation of state very close to the microscopic results of the Illinois group [23]. This can be applied at higher densities, as for instance in neutron stars, with much more confidence than the simple extrapolations of phenomenological functionals, which are adjusted only at the saturation density and below. In

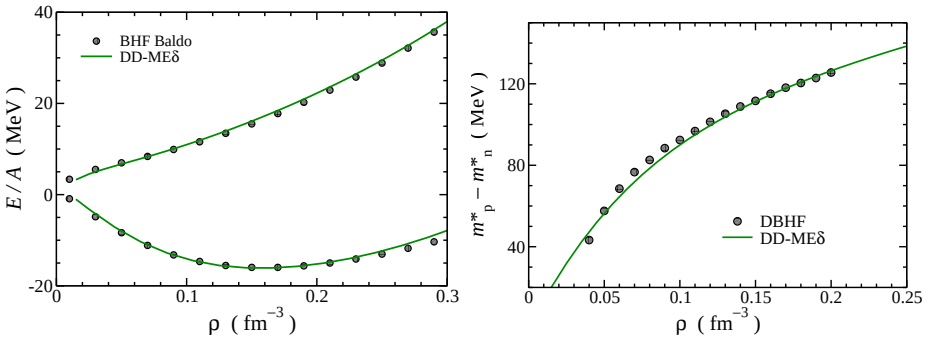

Figure 1. (Color online) Binding energy per nucleon E/A for symmetric nuclear matter and for neutron matter (left panel)and proton-neutron effective mass difference as a function of the nucleon density in pure neutron matter (right panel). The dots represent the results of BHF [17] and RBHF [18, 19] calculations. The lines correspond to DD-MEδ. Figure taken from Ref. [20].

analogy to the non-relativistic considerations of the Catania group [24], a semi-phenomenological covariant functional DD-MEδ has been derived. It contains besides the isovector vector ρ-meson the isovector scalar δ-meson [20] and it is adjusted to the equations of state in symmetric nuclear matter and in neutron matter derived in non-relativistic Brueckner-Hartree-Fock (BHF) theory [17] (see the left panel of Fig. 1) and to the proton-neutron effective mass difference calculated in covariant RBHF calculations [18, 19] (see right panel of Fig. 1). In addition it has only 4 phenomenological parameters for the additional fine-tuning. In fact, for microscopic nuclear energy density functionals, such a fine-tuning will always be necessary.

Looking, for instance, at the various contributions to the total binding energy of ^{208}Pb, one finds for the functionals DD-MEδ and DD-PC1 that the scalar energy E_S of roughly 30 GeV is compensated mainly by the vector energy E_V and by the kinetic energy. The total binding energy E_{tot} of roughly 1.638 GeV represents only $\approx$ 5 % of the scalar energy. Consequently, to reach an accuracy of 100 keV, as required for some astrophysical applications, one needs an accuracy of $0.1/30000 \approx 3 \cdot 10^{-6}$. This will never be reached in ab-initio calculations without some fine-tuning.

A systematic investigation over the entire nuclear chart in Ref. [25] has shown that the semi-microscopic functional DD-MEδ has very similar properties as DD-ME2. This is a remarkable result because compared to DD-ME2 with eight, DD-MEδ has only four phenomenological parameters. The rest is determined ab-initio, i.e., by the bare nucleon-nucleon force through relativistic and non-relativistic Brueckner-Hartree-Fock theory.

3. Relativistic Bruechner-Hartree-Fock theory

Relativistic Brueckner-Hartree-Fock (RBHF) theory is one of the most successful *ab initio* approaches. It is based on bare two-body forces only. On the contrary, in non-relativistic ab initio calculations, one needs three-body forces with additional phenomenological parameters. Recently RBHF theory has also been applied for light finite nuclei [26, 27]. The relativistic framework contains the important Z-diagram [28], an effective three-body force generated by a virtual nucleon-antinucleon excitation.

Since the pioneering work of the Brooklyn group [29, 30], RBHF calculations are primarily performed with positive-energy states (PESs) because the construction of NN interaction matrix elements in entire Dirac space, i.e., between negative-energy states (NESs) and PESs, and the corresponding solution of the in-medium scattering equation is rather complicated. The corresponding computer codes for the relativistic in-medium scattering are usually based on the old relativistic scattering codes in free space [31], where negative energy states are not

necessary. To compensate for the incompleteness of the Dirac space, different approximations have been introduced to extract the effective single-particle potentials [32, 33, 34] necessary for the self-consistent solution of the Hartree-Fock equation. These approximations have been applied to solve for symmetric [32, 35, 33, 34, 36] and asymmetric nuclear matter [37, 38, 39, 40, 41, 18, 42, 43]. However, it turned out that they cannot uniquely determine the single-particle properties [44]. Contradictory results for the isospin dependence of single-particle potentials are found between two frequently used approximations [45]. Therefore, to clarify the properties of asymmetric nuclear matter, it is necessary to solve the RBHF equations in the full Dirac space [46, 47, 48].

Recently, self-consistent RBHF calculations in the full Dirac space have been carried out for SNM [49] and for ANM [50]. They avoid the approximations used in RBHF calculations in the Dirac space with PESs only. The saturation properties found in this way are in good agreement with the empirical values.

In the RBHF theory, the nucleons inside the nuclear medium are viewed as dressed particles because of the interactions with the surrounding nucleons. The single-particle motion of a nucleon with rest mass M, momentum $\boldsymbol{p}$, and single-particle energy $E_{\boldsymbol{p}}$, are found by the solution of the Dirac equation.

$$\left[\boldsymbol{\alpha}\cdot\boldsymbol{p}+\beta\left(M+\Sigma(\boldsymbol{p})\right)\right]\psi(\boldsymbol{p})=E_{\boldsymbol{p}}\psi(\boldsymbol{p}), \tag{1}$$

where Σ is the self-energy in full Dirac space:

$$\Sigma(\boldsymbol{p})=U_S(p)+\gamma^0U_0(p)+\boldsymbol{\gamma}\cdot\hat{\boldsymbol{p}}\,U_V(p). \tag{2}$$

The effective Dirac-mass is given by $M_D(p)=M+U_0(p)$ Here $\hat{\boldsymbol{p}}=\boldsymbol{p}/p$ is the unit vector parallel to the momentum $\boldsymbol{p}$. $U_S(p)$, $U_0(p)$, and $U_V(p)$ are the scalar potential, the timelike part, and the spacelike part of the vector potential. For simplicity, spin and isospin indices are neglected. $\psi(\boldsymbol{p})$ are Dirac spinors. For each value of $\boldsymbol{p}$, there is a solution with positive energy (PES) and one with negative energy (NES). One needs the self-energy in full Dirac space for their calculation.

In the RBHF scheme, the single-particle operator Σ in Dirac space is calculated as integral over the effective relativistic interaction, the G-matrix

$$\Sigma(p)=\int_0^{p_F}\frac{d^3p'}{(2\pi)^3}\langle\bar{\psi}(\boldsymbol{p})\bar{\psi}(\boldsymbol{p'})|\bar{G}(W)|\psi(\boldsymbol{p})\psi(\boldsymbol{p'})\rangle. \tag{3}$$

Here one sums up over all occupied states in the Fermi sea ($|\boldsymbol{p'}|\leq p_F$). For simplicity, spin- and isospin-indices are neglected in these equations. W is the starting energy. For further details, see Ref. [49].

For the calculation of the self-energy in full Dirac space in Eq. (1), one needs all the matrix elements G^{++++}, G^{+-++}, and G^{--++}, where $\pm$ indicate positive and negative energy solutions.

The effective NN interaction G in the nuclear medium is the basic ingredient of RBHF theory. In non-relativistic BHF theory, it is an effective scattering matrix, found as the solution of the Bethe-Goldstone equation [51, 52]. Here the Pauli operator Q excludes scattering processes to occupied states below the Fermi surface.

In relativistic scattering theory, the scattering matrix is determined by the four-dimensional Bethe-Salpeter equation [53]. To reduce it to a three-dimensional equation, several methods have been proposed [54, 55]. Nowadays, in most of the applications of the RBHF scheme, the G-matrix is calculated by solving the in-medium covariant Thompson equation [32],

$$G(\boldsymbol{q'},\boldsymbol{q}|\boldsymbol{P},W)=V(\boldsymbol{q'},\boldsymbol{q}|\boldsymbol{P})+\int\frac{d^3k}{(2\pi)^3}V(\boldsymbol{q'},\boldsymbol{k}|\boldsymbol{P})\frac{Q(\boldsymbol{k},\boldsymbol{P})}{W-E_{\boldsymbol{P}+\boldsymbol{k}}-E_{\boldsymbol{P}-\boldsymbol{k}}}G(\boldsymbol{k},\boldsymbol{q}|\boldsymbol{P},W). \tag{4}$$

Here $\boldsymbol{P} = \frac{1}{2}(\boldsymbol{k}_1 + \boldsymbol{k}_2)$ and $\boldsymbol{k} = \frac{1}{2}(\boldsymbol{k}_1 - \boldsymbol{k}_2)$ are the center-of-mass and the relative momenta of the two interacting nucleons with the momenta $\boldsymbol{k}_1$ and $\boldsymbol{k}_2$. The initial, intermediate, and final relative momenta of the two nucleons are $\boldsymbol{q}, \boldsymbol{k}$, and $\boldsymbol{q}'$. W denotes the starting energy and the Pauli operator $Q(\boldsymbol{k}, \boldsymbol{P})$ restricts the NN scattering in the nuclear medium.

Equations (1), (3), and (4) form a coupled system. It has to be solved by iteration, in a self-consistent way. After convergence, the binding energy per nucleon for ANM can be calculated straightforwardly [40, 42, 43].

In previous RBHF calculations [32, 33, 34] the Thompson equation (4) is solved in the Dirac space with PES only. Because relativistic scattering algorithms are relatively complicated, the starting point for such calculations was the free scattering algorithm used to derive a relativistic NN-potential from the experimental phase shifts [31, 56]. This algorithm is restricted to scattering processes of particles with positive energy. Negative energy solutions (scattering of anti-particles) are not considered. The results of such calculations are the matrix elements of the scattering matrix (T-matrix) and the corresponding phase shifts for proton and neutrons, i.e., for a particle with positive energy. The situation is much more complicated for the self-consistent solution of the RBHF equations. In each step of the iteration, we need, for the evaluation of the Dirac spinors in the medium by the solution of the Dirac equation (1), not only the matrix elements of the potential Σ for PESs Σ^{++}, but also matrix elements Σ^{+-} between PESs and NESs and the elements between NESs Σ^{--}. This requires, in principle, a solution of the Thompson equation (4) in the full Dirac space. Previous RBHF calculations avoid the calculation of Σ^{+-} and Σ^{--}, and use several approximations [32, 33, 34]. It turns out that these approximations are valid for symmetric nuclear matter, but they show significant differences for asymmetric nuclear matter.

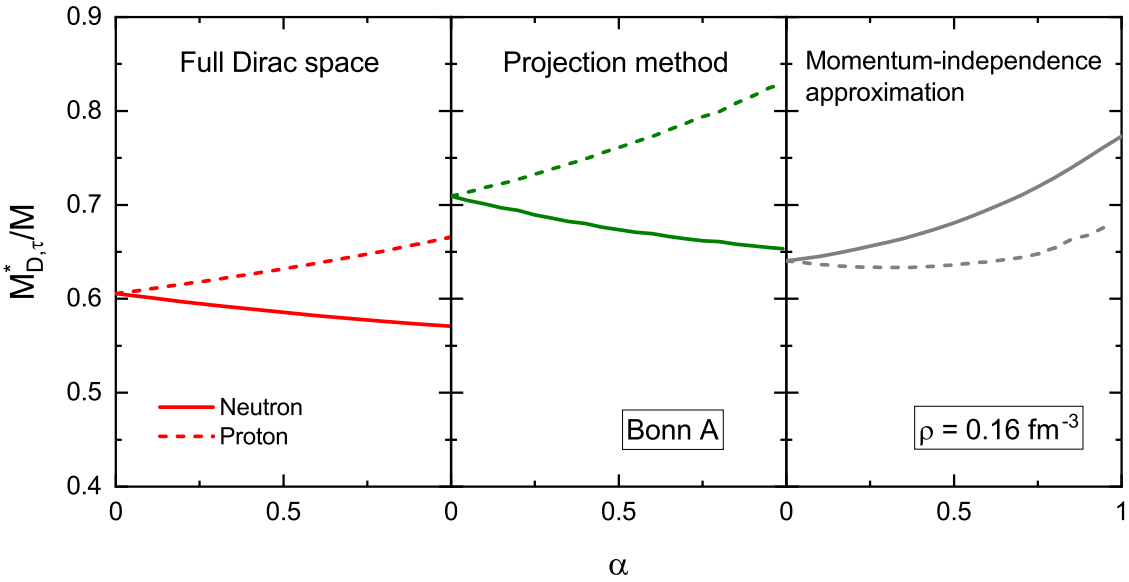

Figure 2. (Color online) Effective Dirac mass for the neutron (solid lines) and the proton (dashed lines) as functions of the asymmetry parameter α at $\rho = 0.16$ fm^{-3} calculated by the RBHF theory in the full Dirac space (left), in comparison with the results obtained by RBHF calculations with PESs only using the projection method [33] (middle) and the momentum-independence approximation [32] (right). The Bonn-A potential [57] is used. Figure taken from Ref. [50].

We investigate the isospin dependence of the single-particle potential. In the left panel

of Fig. 2, the Dirac mass $M^*_{D,\tau} = M + U_{S,\tau}$ at the Fermi surface for protons and neutrons ($\tau = p, n$) obtained with the RBHF theory in the full Dirac space are plotted as functions of the asymmetry parameter $\alpha = (\rho_n - \rho_p)/\rho$ at the density $\rho = 0.16$ fm^{-3}. It is found that, with increasing asymmetry parameter, the Dirac mass for the neutron is decreasing, while for the proton, an opposite tendency is found. As a result, $M^*_{D,n} < M^*_{D,p}$ with the isovector effective mass $(M^*_{D,p} - M^*_{D,n})/M = 0.095$ in pure neutron matter (PNM) is predicted in the full Dirac space.

The other two panels of Fig. 2 contain approximations used in the literature. Here the Thompson equation 4 is solved only for PESs, and the remaining parts of the self-energy $\Sigma(p)$ are determined by various approximations: The middle panel is obtained by the projection method [33] with the *ps* representation for the subtracted T matrix described in detail in Ref. [40].

Comparing with calculations in the full Dirac space, it is found that the projection method leads to a qualitatively consistent isospin dependence of the Dirac mass, but the amplitudes of $M^*_{D,n}$ and $M^*_{D,p}$ are overestimated. The result shown in the right panel of Fig. 2 is obtained with the momentum-independence approximation [32]. Here the spacelike part of the vector potential is neglected, and the momentum dependence of the single-particle potentials is neglected. With these approximations, the scalar potential and the timelike part of the vector potential are extracted directly from the single-particle potential energies at two casually selected momenta, $0.7k^\tau_F$ and k^τ_F. It can be seen that, $M^*_{D,n} > M^*_{D,p}$ for the entire region of the asymmetry parameter. This contradicts the calculations with the RBHF theory in the full Dirac space and with the projection method. As pointed out in Ref. [45], a wrong sign for the isovector dependence of the single-particle potentials is obtained by applying the momentum-independence approximation to asymmetric nuclear systems.

The determination of the single-particle potentials by using the full Dirac space gives us confidence for a reasonable investigation of the symmetry energy and its density dependence. In Fig. 2, the red solid line shows the symmetry energy $E_{\rm sym}(\rho) = \frac{1}{2}\frac{\partial^2 E(\rho,\alpha)}{\partial \alpha^2}\Big|_{\alpha=0}$ found by the RBHF theory in the full Dirac space as a function of the density ρ. At the saturation density $\rho_0 = 0.188$ fm^{-3} (see Ref. [49]), the symmetry energy $E_{\rm sym}(\rho_0)$ is 33.1 MeV. This agrees with the empirical values 31.7 ± 3.2 MeV [61]. The slope parameter of the symmetry energy L is 65.2 MeV, which is consistent with the empirical values 58.7 ± 28.1 MeV [61]. As compared to the results obtained by the projection method (olive dashed line), our results lead to a softer symmetry energy. This fact is also favored by the historical detection of the gravitational wave from GW170817 [62]. The gray band reveals the uncertainties of the momentum-independence approximation as discussed in Ref. [49]. These results demonstrate again that it is important to carry out calculations in the full Dirac space.

The symmetry energy has been extensively studied both in the theory and in the experiment. For the comparison, we consider data from simulations of the low-energy HIC involving ^{112}Sn and ^{124}Sn [58], nuclear structure studies involving excitation energies to isobaric analog states (IASs) [59], and the ASY-EOS experiments at GSI [60]. They are shown as the blue, yellow, and black shadow regions in Fig. 3. Below the saturation density, the symmetry energy obtained by RBHF theory in the full Dirac space is found compatible with the constraints from the IAS [59] and the HIC [58] experiments. At twice normal saturation density, i.e., 0.32 fm^{-3}, the symmetry energy obtained in this work is 51.6 MeV. This is in agreement with the constraint $50.8 - 60.4$ MeV from ASY-EOS [60].

4. Summary

On the way to an ab-initio determination of covariant density functionals, two essential steps forward have been discussed: (a) the determination of the realistic and very successful semi-microscopic functionals DD-PC1 and DD-MEδ has shown that because of essential cancellations

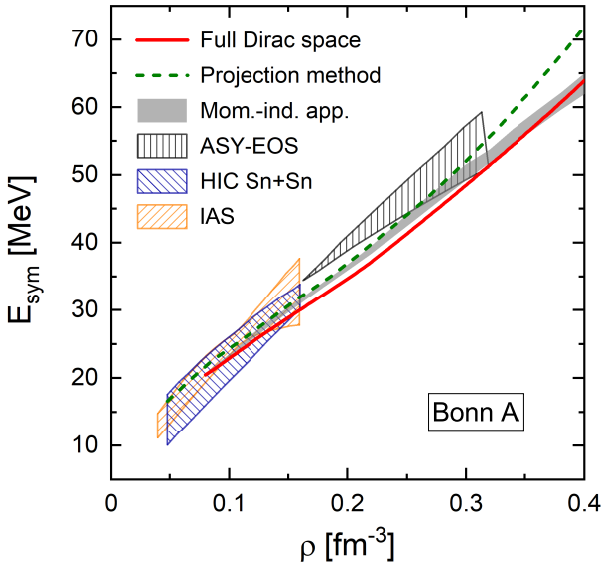

Figure 3. (Color online) The symmetry energy $E_{\rm sym}$ as a function of the density ρ calculated by the RBHF theory in the full Dirac space (red solid line), in comparison with the results obtained by the RBHF calculation with the projection method (olive dashed line) and the momentum-independence approximation (Mom.-ind. app., gray band). The constraints from the HIC [58], the IAS [59], and the ASY-EOS experiments [60] are depicted with blue, yellow, and gray shadows, respectively. Figure taken from Ref. [50].

of the various relativistic potentials, one will always need some fine-tuning to obtain the high required accuracy of the results for binding energies. (b) The problem of solving the Thompson equation in full Dirac space existing for 40 years has been solved. This will allow further steps in an ab-initio derivation of relativistic functionals, such a the derivation of a relativistic version of the potential $V_{\rm lowk}$. The symmetry energy $E_{\rm sym}$ and its slope parameter L at saturation density are 33.1 and 65.2 MeV, respectively, both in agreement with the empirical values. Below saturation density, the symmetry energy is consistent with the experimental constraint of nuclear structure and heavy ion collisions.

5. Acknowledgments

This work was supported in part by the National Key R&D Program of China under Contracts No. 2017YFE0116700 and 2018YFA0404400, the National Natural Science Foundation of China (NSFC) under Grants No. 11935003, No. 11975031, No. 11875075, No. 12070131001, No. 12047564 and No. 12147102, the Fundamental Research Funds for the Central Universities under Grants No. 2020CDJQY-Z003 and No. 2021CDJZYJH-003, the MOST-RIKEN Joint Project "Ab initio investigation in nuclear physics", the Deutsche Forschungsgemeinschaft (DFG, German Research Foundation) under Germany's Excellence Strategy EXC-2094-390783311, ORIGINS, and the Institute for Basic Science (Grant No. IBS-R031-D1). Part of this work was achieved by using the High-performance Computing Platform of Peking University, and the supercomputer OCTOPUS at the Cybermedia Center, Osaka University under the support of Research Center for Nuclear Physics of Osaka University.

References

[1] D. Vautherin and D. M. Brink, Phys. Rev. C **5**, 626 (1972).
[2] J. Dechargé and D. Gogny, Phys. Rev. C **21**, 1568 (1980).
[3] J. Boguta and A. R. Bodmer, Nucl. Phys. A **292**, 413 (1977).
[4] B. D. Serot and J. D. Walecka, Adv. Nucl. Phys. **16**, 1 (1986).
[5] P. Ring, Prog. Part. Nucl. Phys. **37**, 193 (1996).
[6] D. Vretenar, A. V. Afanasjev, G. A. Lalazissis, and P. Ring, Phys. Rep. **409**, 101 (2005).
[7] J. Meng,*et. al.*, Prog. Part. Nucl. Phys. **57**, 470 (2006).
[8] *Relativistic Density Functional for Nuclear Structure*, Vol. 10 of *International Review of Nuclear Physics*, edited by J. Meng (World Scientific, Singapore, 2016).
[9] T. Nikšić, D. Vretenar, and P. Ring, Prog. Part. Nucl. Phys. **66**, 519 (2011).
[10] J. M. Yao, K. Hagino, Z. P. Li, J. Meng, and P. Ring, Phys. Rev. C **89**, 054306 (2014).
[11] P. Ring and E. Litvinova, Phys. At. Nucl. **72**, 1285 (2009).
[12] *Extended Density Functionals in Nuclear Structure Physics*, edited by G. A. Lalazissis, P. Ring, and D. Vretenar (Springer-Verlag, Heidelberg, 2004), Vol. 641.
[13] J. Drut, R. Furnstahl, and L. Platter, Prog. Part. Nucl. Phys. **64**, 120 (2010).
[14] J. P. Perdew and S. Kurth, in *A Primer in Density Functional Theory*, edited by C. Fiolhais, F. Nogueira, and M. A. L. Marques (Springer Berlin), **620**, 1 (2003)
[15] T. D. Cohen, R. J. Furnstahl, K.Griegel, and S.Jin, Prog. Part. Nucl. Phys. **35**, 221 (1995).
[16] H.-P. Dürr, Phys. Rev. **103**, 469 (1956).
[17] M. Baldo, C. Maieron, P. Schuck, and X. Viñas, Nucl. Phys. A **736**, 241 (2004).
[18] E. N. E. van Dalen, C. Fuchs, and A. Faessler, Eur. Phys. J. A **31**, 29 (2007).
[19] E. N. E. van Dalen and H. Müther, Phys. Rev. C **84**, 024320 (2011).
[20] X. Roca-Maza, X. Viñas, M. Centelles, P. Ring, and P. Schuck, Phys. Rev. C **84**, 054309 (2011).
[21] T. Nikšić, D. Vretenar, and P. Ring, Phys. Rev. C **78**, 034318 (2008).
[22] S. Fayans, JETP Lett. **68**, 169 (1998).
[23] A. Akmal, V. R. Pandharipande, and D. G. Ravenhall, Phys. Rev. C **58**, 1804 (1998).
[24] M. Baldo, L. M. Robledo, P. Schuck, and X. Viñas, J. Phys. G **37**, 064015 (2010).
[25] S. E. Agbemava, A. V. Afanasjev, D. Ray, and P. Ring, Phys. Rev. C **89**, 054320 (2014).
[26] S. Shen, J. Hu, H. Liang, J. Meng, P. Ring, and S. Zhang, Chin. Phys. Lett. **33**, 102103 (2016).
[27] S. Shen, H. Liang, W. Long, J. Meng, and P. Ring, Prog. Part. Nucl. Phys. **109**, 103713 (2019).
[28] G. E. Brown, W. Weise, G. Baym, and J. Speth, Comments Nucl. Part. Phys. **17**, 39 (1987).
[29] M. R. Anastasio, L. S. Celenza, and C. M. Shakin, Phys. Rev. Lett. **45**, 2096 (1980).
[30] M. R. Anastasio, L. S. Celenza, and C. M. Shakin, Phys. Rev. C **23**, 2273 (1981).
[31] K. Erkelenz, R. Alzetta, and K. Holinde, Nucl. Phys. A **176**, 413 (1971).
[32] R. Brockmann and R. Machleidt, Phys. Rev. C **42**, 1965 (1990).
[33] T. Gross-Boelting, C. Fuchs, and A. Faessler, Nucl. Phys. A **648**, 105 (1999).
[34] E. Schiller and H. Müther, Eur. Phys. J. A **11**, 15 (2001).
[35] G. Q. Li, R. Machleidt, and R. Brockmann, Phys. Rev. C **45**, 2782 (1992).
[36] C. Wang, J. Hu, Y. Zhang, and H. Shen, J. Phys. G **47**, 105108 (2020).
[37] L. Engvik, M. Hjorth-Jensen, E. Osnes, G. Bao, and E. Østgaard, Phys. Rev. Lett. **73**, 2650 (1994).
[38] Z. Ma and L. Liu, Phys. Rev. C **66**, 024321 (2002).
[39] D. Alonso and F. Sammarruca, Phys. Rev. C **67**, 054301 (2003).
[40] E. N. E. van Dalen, C. Fuchs, and A. Faessler, Nucl. Phys. A **744**, 227 (2004).
[41] F. Sammarruca, W. Barredo, and P. Krastev, Phys. Rev. C **71**, 064306 (2005).
[42] T. Katayama and K. Saito, Phys. Rev. C **88**, 035805 (2013).
[43] H. Tong, X.-L. Ren, P. Ring, S.-H. Shen, S.-B. Wang, and J. Meng, Phys. Rev. C **98**, 054302 (2018).
[44] C. Nuppenau, Y. Lee, and A. MacKellar, Nucl. Phys. A **504**, 839 (1989).
[45] S. Ulrych and H. Müther, Phys. Rev. C **56**, 1788 (1997).
[46] P. Poschenrieder and M. K. Weigel, Phys. Rev. C **38**, 471 (1988).
[47] H. Huber, F. Weber, and M. K. Weigel, Phys. Rev. C **51**, 1790 (1995).
[48] F. de Jong and H. Lenske, Phys. Rev. C **58**, 890 (1998).
[49] S. Wang, Q. Zhao, P. Ring, and J. Meng, Phys. Rev. C **103**, 054319 (2021).
[50] S. Wang, H. Tong, Q. Zhao, C. Wang, P. Ring, and J. Meng, Phys. Rev. C **106**, L021305 (2022).
[51] H. A. Bethe and J. Goldstone, Proc. Roy. Soc. A **238**, 551 (1957).
[52] K. A. Brueckner and J. L. Gammel, Phys. Rev. **109**, 1023 (1958).
[53] E. E. Salpeter and H. A. Bethe, Phys. Rev. **84**, 1232 (1951).
[54] R. Blankenbecler and R. Sugar, Phys. Rev. **142**, 1051 (1966).
[55] R. H. Thompson, Phys. Rev. D **1**, 110 (1970).

[56] K. Erkelenz, Phys. Rep. **13**, 191 (1974).
[57] R. Machleidt, Adv. Nucl. Phys. **19**, 189 (1989).
[58] M. B. Tsang, Y. Zhang, P. Danielewicz, M. Famiano, Z. Li, W. G. Lynch, and A. W. Steiner, Phys. Rev. Lett. **102**, 122701 (2009).
[59] P. Danielewicz and J. Lee, Nucl. Phys. A **922**, 1 (2014).
[60] P. Russotto, M. D. Cozma and A. Le Fevre and Y. Leifels and R. Lemmon and Q. Li, J. Lukasik, and W. Trautmann, Phys. Rev. C **94**, 034608 (2016).
[61] M. Oertel, M. Hempel, T. Klähn, and S. Typel, Rev. Mod. Phys. **89**, 015007 (2017).
[62] B. P. Abbott et al., Phys. Rev. Lett. **119**, 161101 (2017).